PCP- and SCS-Pincer Palladium Complexes Immobilized on Mesoporous Silica: Application in C−C Bond Formation Reactions

Nilesh C. Mehendale,[a] Jelle R. A. Sietsma,[b] Krijn P. de Jong,[b] Cornelis A. van Walree,[a] Robertus J. M. Klein Gebbink,[a] and Gerard van Koten[a,*]

[a] Organic Chemistry and Catalysis, Faculty of Science, Utrecht University, Padualaan 8, 3584 CH Utrecht, The Netherlands
Fax: (+31)-30-252-3615; e-mail: G.vankoten@uu.nl

[b] Inorganic Chemistry and Catalysis, Faculty of Science, Utrecht University, P.O. Box 80 083, 3508 TB Utrecht, The Netherlands

Dedicated to Prof. Dr. Jan-E. Bäckvall on the occasion of his 60th birthday.

Abstract: ECE-pincer palladium(II) complexes {ECE = [$C_6H_3(CH_2E)_2$-2,6]$^-$, E = PPh_2 and SPh} tethered to a trialkoxysilane moiety through a carbamate linkage were immobilized on ordered mesoporous silicas SBA-15 and MCM-41 using a grafting process. The resulting hybrid materials were characterized by IR spectroscopy, solid-state CP/MAS NMR (^{13}C, ^{31}P, and ^{29}Si), and elemental analyses. These analyses showed the integrity of the pincer-metal complexes on the supports, which highlights their stability under the applied immobilization conditions. An H-bonding interaction between the carbamate carbonyl group of the complex and free silanol groups on the silica surface was also established. The hybrid materials were found to act as Lewis acid catalysts in the aldol reaction between methyl isocyanoacetate and benzaldehyde. SBA-15 modified with the PCP-pincer Pd complex was used in up to five runs without loss of activity. Control experiments showed the true heterogeneous nature of the catalyst in this reaction. Nitrogen physisorption data, XRD, and TEM/EDX analyses of the hybrid materials revealed that the mesoporous structure of these materials was retained during the immobilization process as well as during catalysis.

Keywords: aldol reaction; catalyst recycling; immobilization; MCM-41; pincer complexes; SBA-15
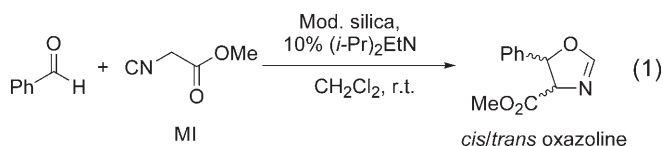
Introduction

Catalyst separation from the product solution is an important aspect of homogeneous catalytic processes both from an economical and ecological point of view. Amongst current methods to separate homogeneous catalysts from product streams are distillation and selective extraction of products and catalysts.[1] In many cases these methods may turn out as unsustainable, however, due to the excessive use of energy and solvents, and could, therefore, also be economically less attractive. In this respect, heterogeneous catalytic processes have obvious advantages due to the ease of separation of the (insoluble) heterogeneous catalysts from reaction products. Current research is directed to merge the advantages of both catalytic approaches, for example, by immobilizing homogeneous catalysts on an insoluble support.[2,3] In this way, properties such as catalyst selectivity and activity could be combined with ease of catalyst separation and catalyst reuse. A variety of insoluble supports has been used for the immobilization of homogeneous catalysts.[4,5]

ECE-pincer metal complexes {ECE = [C_6H_3($CH_2E)_2$-2,6]$^-$, E = NR_2, SR, PR_2 etc.} are often highly stable and resistant to metal leaching due to a strong M−C σ-bond that is stabilized through metal coordination by two heteroatoms (*cis* to the M−C bond) forming two five-membered chelate rings.[6] ECE-pincer Pd complexes are known to catalyze a large variety of C−C and C−X bond formation reactions.[6–10] The robustness of the ECE-pincer metal complexes make them attractive candidates for processes for which recycling and reuse is a prerequisite. Various soluble supports have already been used for the immobilization and recycling of pincer-based metal catalysts, among which are hyperbranched polymers,[9,11] oligo(ethylene glycol),[12] dendronized polymers,[13] carbosilane dendrimers,[14] cartwheel molecules,[8,15] polycationic dendrimers,[16] and soluble polymers.[10,17] Recently, we as well as others have reported on the grafting of ECE-pincer metal complexes on

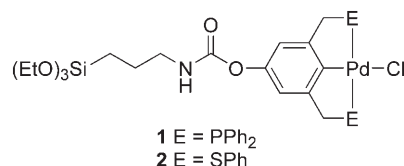silica and on their use in aldol-type[18,19] and Heck re-actions.[20]

In a recent effort by our group to immobilize NCN-pincer complexes on insoluble supports, we have used *para*-triethoxysilane-functionalized pincer-metal (platinum and palladium) complexes and immobilized these on conventional silica gel *via* surface grafting.[18] Although the heterogenized pincer Pd complexes were found to be active in the aldol reaction of methyl isocyanoacetate (MI) with benzaldehyde [Eq. (1)], they showed a poor performance in terms of re-

Figure 1. Siloxane-functionalized ECE-pincer palladium(II) chloride complexes.

$$ Ph-CHO + CN-CH_2-CO_2Me \xrightarrow[\text{CH}_2\text{Cl}_2, \text{ r.t.}]{\substack{\text{Mod. silica,}\\ 10\% (i\text{-Pr})_2\text{EtN}}} \text{cis/trans oxazoline} \quad (1) $$

MI

cycling. For a series of conventional silicas differing in macroscopic particle size (50 μm–1.5 mm) and pore diameter (15–50 nm) significant activity losses of more than 50% between the first and second run were observed for the heterogenized catalysts. No indication could be derived for a relation between the macroscopic particle size and average pore diameter of the silicas, and the degree of catalyst leaching from the support. Presumably during the reaction, attrition of the catalyst took place due to partial hydrolysis of the silica surface. As a result, part of the catalyst was removed from the support in the form of small, difficult to separate by filtration and thus non-recyclable silica particles.

Recent investigations on the mechanism of operation of ECE-pincer palladium(II) complexes as homogeneous catalyst have shown that the NCN- and SCS-pincer Pd complexes undergo isocyanide insertion in the Pd−C bond and that the resulting cyclometalated species are the actual catalytically active species.[21] Remarkably, this insertion takes place for both the neutral halide and the cationic aquo complexes. For the PCP-pincer Pd complexes, no insertion was observed, but replacement of the halide by a η^1-coordinated isocyanide generated the cationic, catalytically active species. Finally, this study showed that there is no need to generate a cationic palladium(II) species by prior treatment of the neutral species with, for example, Ag reagents (note that Ag halide salts are catalysts themselves)[22] for the ECE-pincer palladium species to catalyze the reaction of Eq. (1).

In the present study, we have used our experience to immobilize NCN-pincer palladium complexes for the immobilization of the corresponding PCP- and SCS-pincer palladium complexes on silica.[18] To this end, complexes **1** and **2** (Figure 1) were synthesized[23] and subsequently immobilized on silica-based support materials. The choice of support depended on the re-

action conditions, ease of functionalization of the surface groups required for attaching the catalyst, as well as on the chemical, mechanical and thermal stability of the support.[5] In the present study, we have used the ordered mesoporous molecular sieves MCM-41[24] and SBA-15,[25] which fulfill most of the above-mentioned requirements and have been used extensively by others.[3,26] Moreover, their well-defined structure may provide uniform active sites with well-controlled steric effects of the support.[27] The synthesis and characterization of the pincer palladium-functionalized MCM-41 and SBA-15 materials as well as their performance in the reaction of Eq. (1) are discussed.

Results and Discussion

Immobilization of PCP- and SCS-Pincer Palladium Complexes on Silica

The triethoxysilane-functionalized complexes **1** and **2** (Figure 1) were prepared from the corresponding *para*-hydroxy ECE-pincer complexes as reported previously.[23] These complexes comprise both a trialkoxysilane and an organometallic fragment covalently connected through a carbamate linker. The presence of a long, non-polar tail increases the solubility of these complexes considerably. They are soluble in non-polar solvents such as benzene or toluene, which allows the use of common grafting protocols of homogeneous catalysts on silica in these solvents. This is of importance to arrive at a uniform distribution of the catalyst on the support.

Silica surface grafting of **1** and **2** was carried out using SBA-15 or MCM-41. In a typical process, the silica support was pre-treated by heating it at 100°C under vacuum for two hours. The support was then reacted with complexes **1** or **2** in toluene at 90°C for 20 h (Scheme 1). A continuous extraction (Soxhlet) of the resulting material with boiling dichloromethane was subsequently performed for 16 h in order to remove any non-covalently attached material. After drying under vacuum, the hybrid silicas **3** and **4**, respectively, were obtained as white solids. Subsequently, silica **3** was treated with 1,1,1,3,3,3-hexamethyldisilazane (HMDS) to cap remaining unreacted surface silanol groups with a trimethylsilyl functionality (silica **5**).
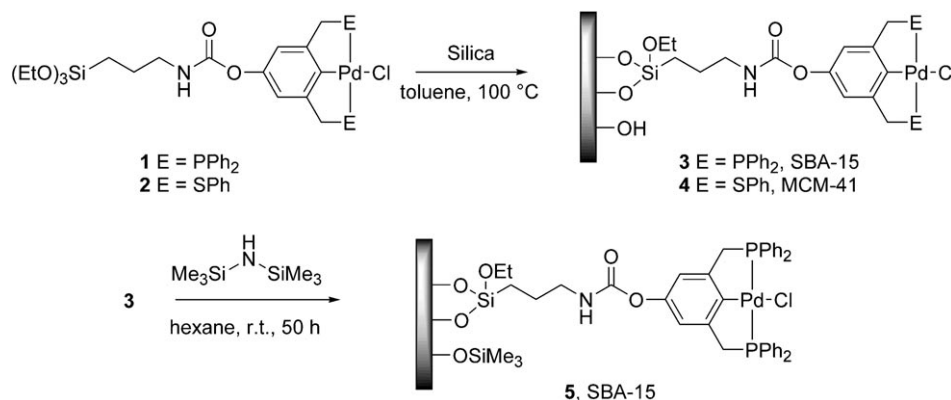
Scheme 1. Synthesis of hybrid materials **3**, **4**, and **5**.

These materials were characterized by using IR spectroscopy (DRIFT), CP/MAS NMR spectroscopy (^{13}C, ^{29}Si, and ^{31}P), and elemental analysis. The impact of the immobilization of **1** and **2** on the structure of MCM-41 and SBA-15 was studied by powder X-ray diffraction (XRD), transmission electron microscopy (TEM), and nitrogen physisorption.

Characterization

IR Studies

Comparison of the IR (DRIFT) spectra of the pristine silicas (SBA-15 in Figure 2) with those of hybrid materials **3** (see Figure 2) and **4** pointed to a strong decrease in the number of isolated free silanol groups in the latter silicas. Comparison of the IR spectra of **1** and **2** with those of the hybrid materials **3** and **4** revealed that signals corresponding to the C−H stretching, C=O stretching, CNH group, and the N−H bending vibrations of **1** and **2** are present in the spectra of **3** and **4**. The intensity of the signal for isolated free silanol groups in **3** is further decreased in the spectrum of **5** (see Figure 2), showing that at least part of the remaining silanol groups in **3** became capped with a TMS group in **5**. By subtracting the spectrum of plain SBA-15 from that of **5**, a difference spectrum was obtained (*top*, Figure 3). In this difference spectrum, a sharp decrease in the intensity of the signal at 3745 cm^{-1} was observed indicating that a large number of silanol groups had reacted. Other significant changes were observed for the carbamate C=O stretching vibration. In **1** the $\tilde{v}$(C=O) amounted to 1734 cm^{-1} (see Figure 3), which changed to 1725 cm^{-1} in hybrid material **3**, and to 1756 cm^{-1} in TMS-capped **5** (see Figure 2).

We believe that these shifts are indicative for the presence of H-bonding interactions of the carbamate carbonyl group with surface silanol groups in **3**, which consequently are much less present in **5**. This observa-

tion is consistent with previous observations made on immobilizing related NCN-pincer complexes on silica.[18]
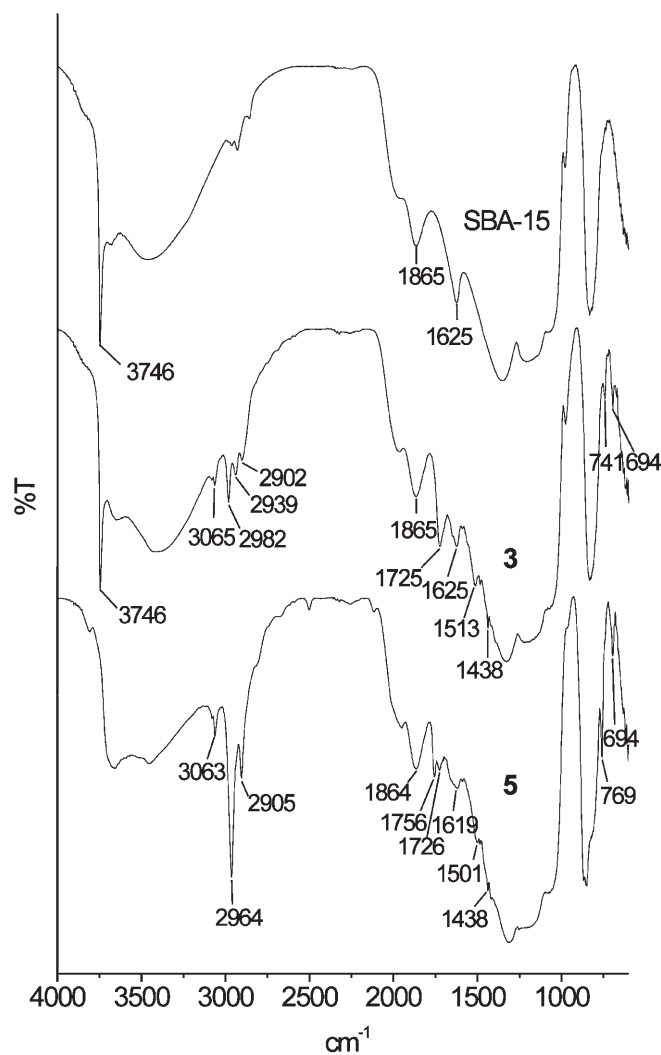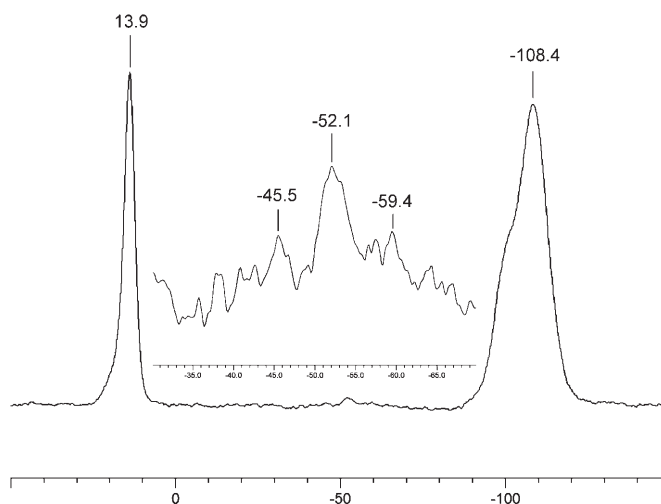

Figure 2. IR (DRIFT) of plain silica (SBA-15) and hybrid materials **3** and **5**.
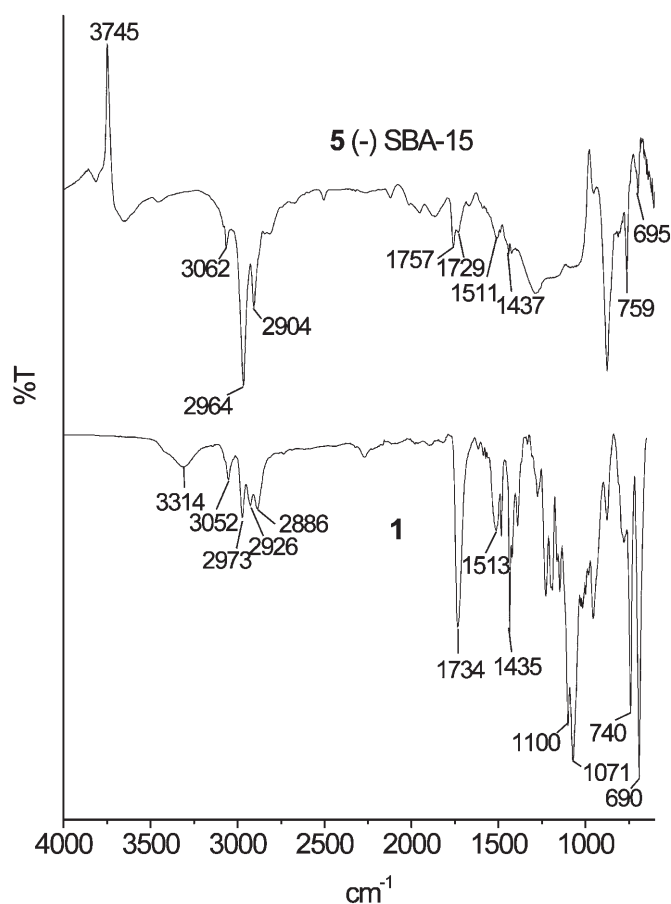
Figure 3. Difference spectrum between the DRIFT spectra of **5** and SBA-15 (*top*) compared with IR spectrum of non-supported **1** (*bottom*).

Figure 4. CP/MAS solid-state ^{29}Si NMR of **5** (inset: expansion of -30 to -70 ppm region).

and -45 ppm, corresponding to T^3, T^2, and T^1 types of organosilica species, respectively [Figure 4, inset; $T^n = RSi(OSi)_n(OEt)_{3-n}$].

In addition, the latter spectrum also showed a signal at 13.9 ppm, which can be assigned to Si-(surface)$-$O$-$SiMe$_3$ groups derived from surface silanols capped with a Me$_3$Si grouping arising from HMDS treatment of the hybrid material **3**.[28] Two signals were observed for the SiO$_2$ framework of **3** at -108 and -101 ppm, respectively, corresponding to Q^4 and Q^3 species [$Q^m = Si(OSi)_m(OH)_{4-m}$], whereas for **5** a signal at -108 ppm (Q^4 species) along with a shoulder at about -100 ppm (decreased number of Q^3 species) was observed, which is in accordance with the partial SiMe$_3$ capping of silanol groups (Q^3 species) in **5** (*vide supra*).

CP/MAS Solid State NMR Studies

^{13}C and ^{29}Si solid-state NMR spectroscopy on **3**, **4**, and **5** provided further information on the nature of both the organic (spacer and metal-complex) and inorganic part of these hybrid materials. All peaks corresponding to the ^{13}C NMR spectra of the parent complexes **1** and **2** were present in the ^{13}C NMR spectra of the hybrid materials **3** and **4**, respectively. The ^{31}P NMR spectrum of solid **3** (on SBA-15) showed a single peak at 36.01 ppm, while for **1** a resonance at 33.4 ppm (solution NMR in C$_6$D$_6$) was found which corresponds to a phosphine grouping coordinated to palladium. Signals at 16 and 58 ppm in the ^{13}C NMR spectra of all hybrid materials pointed to the presence of EtO$-$Si groups.[23] This supports the notion that not all tethered palladium complexes became immobilized *via* three Si(surface)$-$O$-$Si bonds, but rather that grafting occurred through an average of less than or equal to three bonds. The ^{29}Si NMR spectrum of **5** indeed showed all three T^n type signals at -59, -52,

Elemental Analysis

The palladium, sulfur, phosphorus, and carbon contents of the grafted silicas were determined by ICP analysis (Table 1). The E/Pd ratio (E = S or P) was close to two for **4** as expected from its formula. In the case of **3** and **5**, this ratio was found to be higher than two, which could point to loss of Pd from the PCP-pincer ligand during the grafting process. ^{31}P NMR analysis of these materials did, however, not show the presence of free phosphine or of phosphine oxide moieties. In addition, no Pd(0) formation was observed during the immobilization reaction, which justifies the conclusion that the complex remained intact. In the case of **5**, an increase of the carbon content was found, which most likely is due to the capping of part of the free silanol groups of SBA-15 with SiMe$_3$ groups.

Table 1. Elemental analyses of the hybrid materials **3–5**.

Sample	Wt. % C[a] (mmol g)$^{-1}$[b]	Wt. % Pd (mmol g^{-1})	Wt. % E[c] (mmol g^{-1})	E/Pd[d] Calc.	Found	C/E[d] Calc.	Found
3	4.96 (4.13)	0.82 (0.077)	0.85 (0.275)	2.0	3.6	18	15
4	1.71 (1.43)	0.43 (0.040)	0.28 (0.087)	2.0	2.2	15	16
5	7.66 (6.38)	0.57 (0.054)	0.58 (0.187)	2.0	3.4	-	-

[a] % by weight.
[b] In brackets, mmol per gram silica.
[c] E = S for SCS and P for PCP.
[d] Atom ratio.

Nitrogen Physisorption

In order to gather information on changes in surface properties at various stages of the synthesis of silicas **3**, **4** and **5**, the materials were studied using nitrogen physisorption. The results are summarized in Table 2 and some selected isotherms are shown in Figure 5.

To ascertain the effect of the conditions of the immobilization process on the ordered structure of SBA-15, we refluxed pristine SBA-15 at 85 °C in toluene for 24 h. The nitrogen physisorption isotherm (Figure 5a) of the obtained product contained the typical features: a high onset at low relative pressures originating from the intra-wall microporosity, and hysteresis at higher values because of the ordered mesoporous channels. The small relative pressure region ($p/p_o = 0.69$–0.71) in which the single-step capillary condensation took place is a consequence of the uniform mesopore diameter of 8.7 nm. The BET surface area and mesopore volume remained unaffected by the treatment (entry 2, Table 2). Next, the impact of the silanol capping treatment with HMDS was addressed by treating blank SBA-15. The isotherm (Figure 5a) showed that the characteristic SBA-15 features were retained.

However, the porosity and average pore size diameter had decreased to 0.49 cm^{3}g^{-1} SiO$_2$ and 7.8 nm, respectively (entry 3, Table 2). The observed pore diameter decrease could not account for the total porosity decrease, and most likely some of mesopores of SBA-15 became blocked. In addition, after the HMDS treatment no micropore volume was present anymore. Comparison of the nitrogen physisorption results of pristine SBA-15 and functionalized material **3** showed that the BET surface area and mesopore volume decreased from 518 to 442 m^{2}g^{-1} SiO$_2$, and from 0.73 to 0.62 cm^{3}g^{-1} SiO$_2$, respectively (entry 4, Table 2). The mesopore diameter had decreased from 8.7 to 8.2 nm due to immobilization of complex **1** inside the mesopores of SBA-15. The steep capillary condensation step and hysteresis loop of the isotherm (Figure 5b) showed that the uniform character of the cylindrical mesopores had been retained. The observed mesoporosity reasonably matched the expected value of 0.58 cm^{3}g^{-1} due to the pore diameter decrease of 0.5 nm. Comparison of the textural properties of materials **3** and **5** showed that treatment of **3** with HMDS resulted in a decline of the micropore volume from 0.05 to 0.00 cm^{3}g^{-1} SiO$_2$, and a further decrease of the mesoporosity to 0.47 cm^{3}g^{-1} SiO$_2$

Table 2. Nitrogen physisorption data of functionalized silica materials.

|	Material	S$_{BET}$[a] [m^2·g^{-1} SiO$_2$]	d$_{pore}$[b] [nm]	V$_{micro}$[c] [cm^3·g^{-1} SiO$_2$]	V$_{meso}$[d] [cm^3·g^{-1} SiO$_2$]	V$_{tot}$[e] [cm^3·g^{-1} SiO$_2$]
1	SBA-15	518	8.7	0.09	0.73	0.78
2	SBA-15 (toluene)	504	8.7	0.09	0.71	0.75
3	SBA-15 (HMDS)	460	7.8	0.00	0.49	0.54
4	**3**	442	8.2	0.05	0.62	0.66
5	**5**	433	7.9	0.00	0.47	0.51
6	**5** after run 1	416	7.9	0.00	0.45	0.49
7	**5** after run 5	423	7.9	0.00	0.46	0.50
8	MCM-41	975	4.3	0.01	0.86	1.03
9	**4**	966	4.1	0.00	0.76	0.95

[a] S$_{BET}$ = BET surface area.
[b] d$_{pore}$ = average pore diameter calculated using NL-DFT.
[c] V$_{micro}$ = micropore volume.
[d] V$_{meso}$ = mesopore volume.
[e] V$_{tot}$ = total pore volume determined at $p/p_o = 0.995$.
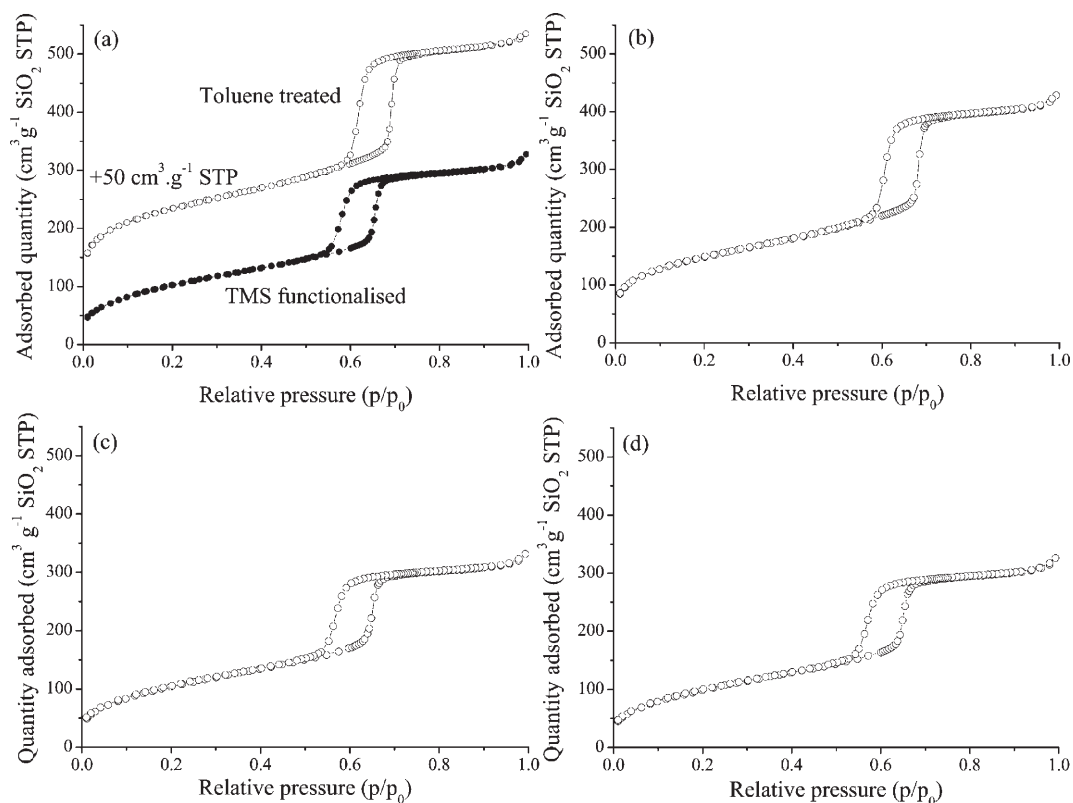
Figure 5. Nitrogen physisorption isotherms of SBA-15 after toluene or HMDS treatment (**a**), functionalized material **3** (**b**) and **5** (**c**), and **5** after five catalytic runs (**d**).

(entry 5, Table 2). Finally, nitrogen physisorption results obtained after catalysis with material **5** (Figure 5d) showed that the textural properties remained unchanged up to five catalytic runs.

The physisorption results in Table 2 (entries 8 and 9) show that immobilization of the SCS-pincer metal complex **2** onto MCM-41, yielding functionalized material **4**, had little effect on the surface area and total pore volume of the support. Also, the steep capillary condensation mesopore-filling step characteristic for cylindrically shaped mesopores was retained. Although the narrow pore size distribution had been preserved the pore diameter had slightly decreased from 4.3 to 4.1 nm upon immobilization of SCS-pincer metal complex **2**.

XRD Analysis

The X-ray diffraction patterns for SBA-15 and corresponding hybrid materials are shown in Figure 6 A. The pattern of pristine SBA-15 revealed three well-resolved peaks located at 1.15, 2.0, and 2.3 degrees 2θ, that could be indexed as the (100), (110) and (200) diffraction lines, respectively, associated with a *p6mm* hexagonal symmetry that is typical for SBA-15. Although small variations between the d-spacing values

of the (100) diffraction line of the different samples were found, the XRD results demonstrated that the hexagonal symmetry was retained for all the functionalized materials; not only after immobilization of the complex and HMDS capping of the remaining hydroxys, but also after five runs of catalysis.

The XRD patterns for blank MCM-41 contained four diffraction lines at 2.1, 3.7, 4.2, and 5.6 degrees 2θ. Again, these could be assigned to the (100), (110), (200) and (210) lattices of the hexagonal lattice of MCM-41, respectively (Figure 6 B). Comparison between the patterns obtained for pristine MCM-41 and functionalized material **4** shows that the long-range order of the mesopores was not affected by the grafting treatment.

TEM/EDX Analysis

TEM analysis of samples of **3** and **5** (SBA-15 materials, Figure 7) as well as of **4** (MCM-41 material; not shown) revealed that the hexagonal mesoporous structures of both SBA-15 and MCM-41 had been retained during immobilization and consecutive steps in the preparation. Figure 7 shows two typical TEM images of material **5** before catalysis and after five catalytic runs. The images demonstrate that the or-
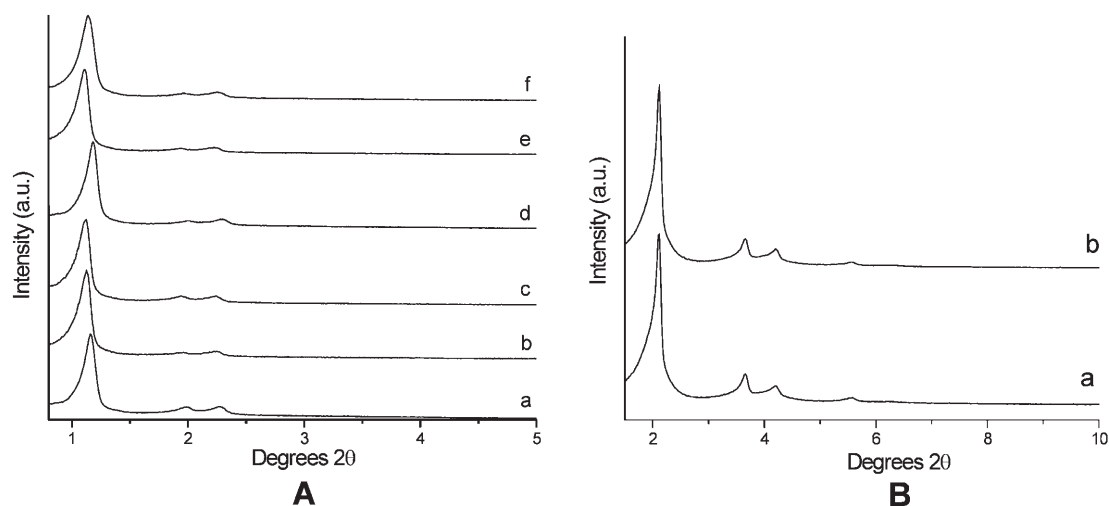
Figure 6. A: XRD patterns of (**a**) SBA-15, (**b**) SBA-15(HMDS), (**c**) **3**, (**d**) **5**, (**e**) **5** after run 1 and (**f**) **5** after run 5; **B:** XRD patterns of (**a**) MCM-41 and (**b**) hybrid material **4**.
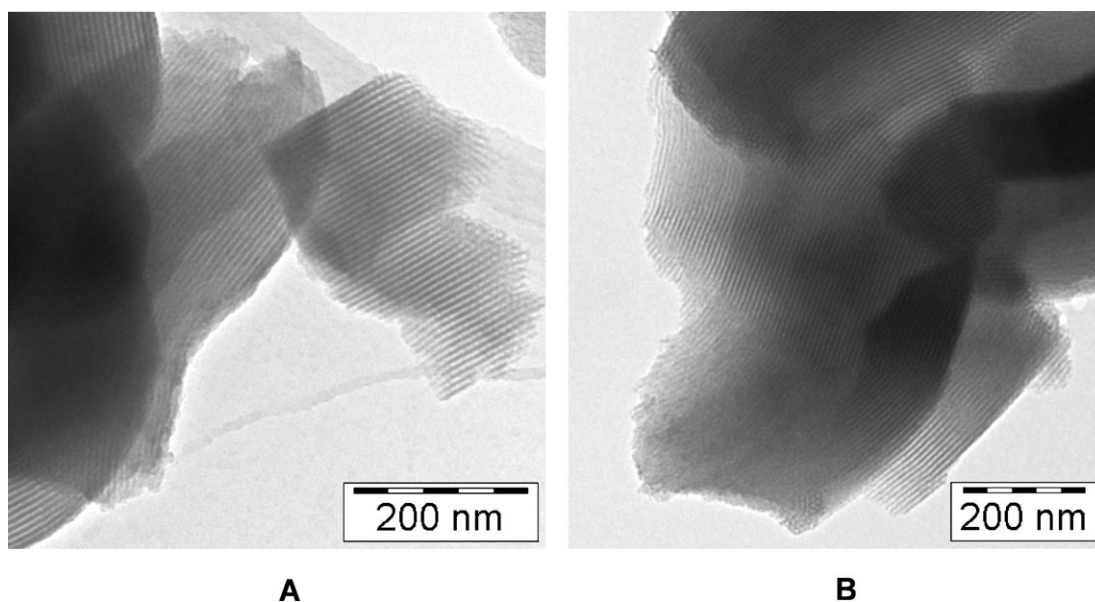
Figure 7. TEM of functionalized SBA-15 **5** (**A**) and **5** after catalysis run 5 (**B**).

dered structure of the SBA-15 was retained. Moreover, with TEM no palladium clusters were found in the samples, however, EDX elemental analysis demonstrated that palladium as well as either phosphorous (for **3** and **5**) or sulfur (for **4**) are present in the structures. This indicated that no Pd(0) was formed during the immobilization and protection processes and that the organometallic groupings **1** and **2** have been molecularly immobilized.
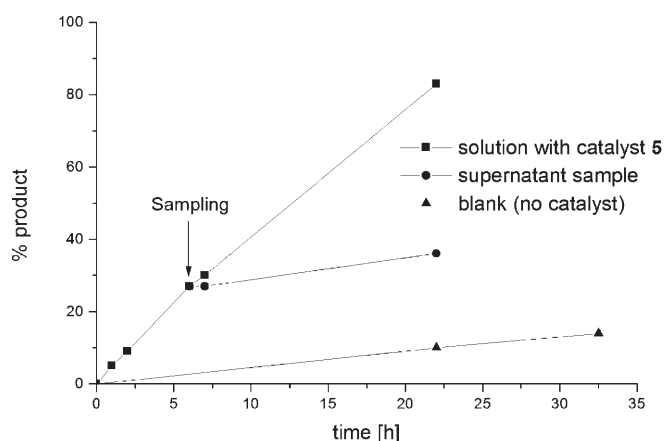
Catalysis

As a test reaction for the catalytic properties of the hybrid materials **3**–**5**, the earlier studied aldol conden-

sation reaction between benzaldehyde and MI [Eq. (1)] was chosen. For this reaction the ECE-pincer palladium(II) halide complexes can be used as such (see Introduction).[21]

As a proof of principle, 250 mg of silica **5** which correspond to 0.84 mol% of palladium loading were tested. Catalysis using 1.6 mmols of both benzaldehyde and MI was run to 30% conversion (Figure 8).

At this stage stirring was stopped and a small part of the clear supernatant solution was removed and stirred separately. At the same time stirring of the remaining reaction mixture was continued. It was found that in the latter reaction mixture, catalysis in the presence of the hybrid material went further to completion, whereas the rate of the reaction in the sample
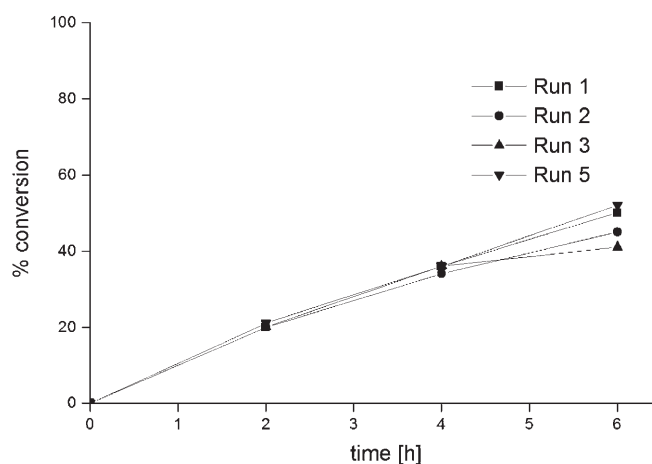
Figure 8. Kinetic traces of aldol reaction [Eq. (1)], showing catalysis only in the presence of silica **5**; the supernatant sample (see text) shows the same kinetic trace as the blank.

Figure 9. Consecutive use of silica **5** in reaction of Eq. (1).

of the supernatant had considerably slowed down and had become comparable to that of the blank reaction (Figure 8), i.e., that of a homogeneous reaction without added ECE-pincer Pd complex. These observations indicate that the activity in the parent reaction and in the reaction mixture after sampling is associated with the catalytic activity of the (insoluble) hybrid material, i.e., with Pd catalysis of the grafted PCP catalyst, thereby demonstrating the true heterogeneous nature of the catalyst.

Next, the recyclability of hybrid material **5** as catalyst for the reaction of Eq. (1) was investigated. In this series of experiments, 500 mg of **5**, which correspond to 1.67 mol% of palladium loading, were used. Again 1.6 mmols of both benzaldehyde and MI were utilized. Work-up in between cycles involved centrifugation of the reaction mixture to separate the suspended silica and removal of the clear supernatant solution. The silica was washed twice with dichloromethane and then reused in the subsequent run. In total five consecutive runs were carried out. It was found that the activity of the catalyst was fully retained over these runs (Table 3, Figure 9). Comparison of the rate of the aldol reaction catalyzed by homogeneous PCP-pincer palladium complex [PdCl(PCP)] with that of the hybrid material **5** showed that the homogeneous

reaction (initial TOF 15 h^{-1}) was faster than the heterogeneous one (initial TOF 6 h^{-1}).

The supernatant reaction mixture for each of these runs was tested for palladium and silicon contents (Table 4). Some leaching of Pd on the ppm level was

Table 4. Elemental analyses of supernatant aldol reaction mixtures catalyzed by **5**.

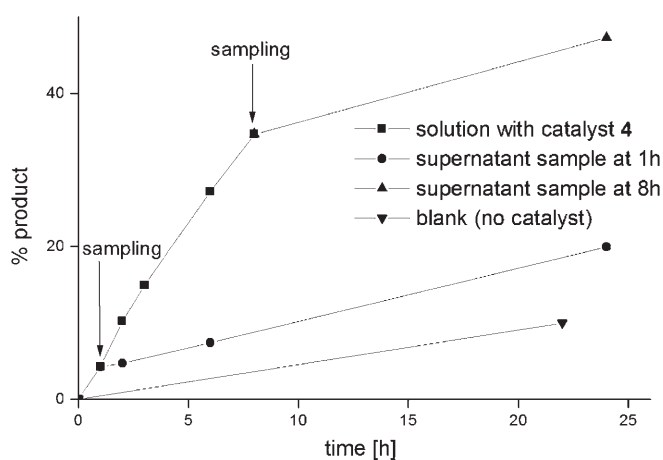| Sample	ppm Pd	ppm Si	Molar ratio Si/Pd
Run 1	348	856	9.3
Run 2	126	969	29.1
Run 3	144	728	19.1
Run 4	96	113	4.5
Run 5	115	447	14.7

found but also the presence of Si was observed in the supernatant solutions. The amount of Si was larger as compared to that of Pd. This indicates that the origin of Pd is probably not the complex (which has a Pd/Si ratio of 1) but rather some small particles of silica itself that escaped separation from the solution. Moreover, the fact that the activity remained constant after each run indicated that leaching of the catalytic species during these experiments was negligible.

TEM analyses carried out on a sample of **5** after run 1 and after run 5 indicated that the structure of the SBA-15 support was not damaged during catalysis. Furthermore, zerovalent palladium clusters were not observed in any of the investigated samples, i.e., no decomposition had occurred. EDX measurements confirmed that palladium and phosphorus were present in the samples, supporting the presence of the PCP-pincer Pd complex. Further evidence for the integrity and stability of the hybrid material **5** after using it in the aldol reaction [Eq. (1)] over 5 runs

Table 3. Consecutive use of silica **5** in reaction of Eq. (1).

Run	% conversion after				*trans* product
	2 h	4 h	6 h	24 h	
1	20	36	50	-	83%
2	20	34	45	-	84%
3	20	36	41	96	84%
4	-	-	-	96	84%
5	21	36	52	92	83%

comes from solid-state ^{31}P NMR, which showed a single peak at 42.3 ppm. This chemical shift corresponds to that of the P-centre in a cationic PCP-pincer Pd-complex with a coordinated isocyanide ligand instead of a chloride as the fourth ligand. This is consistent with our findings in case of the corresponding homogeneous complex, i.e., in a reaction of neutral [PdCl(PCP)] with MI, the ^{31}P NMR resonance shifts from 31 ppm (neutral complex) to 42 ppm (cationic complex [Pd(PCP)(MI)]Cl).[21]

Hybrid material **4** (with the SCS-pincer palladium grouping) was found to behave in a similar manner as **5**. Similar experiments involving about 200 mg of silica **4** (0.48 mol% of palladium loading) confirmed that catalysis in the first run took place only because of the presence of **4** (Figure 10). However, upon recy-

Figure 10. Aldol reaction of Eq. (1) catalyzed by silica **4**.

cling of **4**, a decreased activity was found. This is most likely due to catalyst deactivation and can be attributed to a low stability of the insertion complex that is formed upon reaction of SCS-pincer Pd complex with an isocyanide [see Eq. (2)]. Such insertion complexes are not formed in the case of PCP-pincer Pd complexes[21] and, consequently, no deactivation is observed for hybrid materials derived from these complexes, i.e., for **3** and **5**. In the case of hybrid material **4**, a lower initial TOF of 11 h^{-1} was observed whereas with its homogeneous counterpart SCS-pincer palladium complex [PdCl(SCS)] an initial TOF of 45 h^{-1} was found.
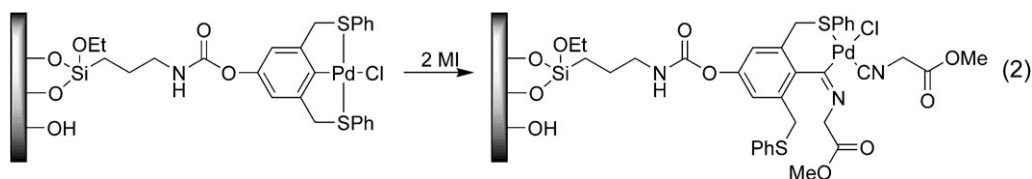
Conclusions

We have shown that ECE-pincer Pd complexes were successfully immobilized on ordered mesoporous silicas. During immobilization the integrity of both the organometallic moiety and the inorganic support remained unchanged. It was found that hybrid mesoporous material **5** derived from PCP-pincer palladium complex showed a good activity and recycling ability, whereas the corresponding hybrid mesoporous material **4** with the SCS-pincer palladium complex, in spite of showing a similar initial activity in the first run, had a poor recycling ability. Likewise, a good initial activity together with a poor recycling ability was observed in the experiments with immobilized NCN-pincer palladium compounds.[18] It must be noted that both NCN- and SCS-pincer palladium complexes undergo a selective insertion reaction with MI, cf. Eq. (2). As the corresponding PCP-pincer Pd complex does not suffer from such an insertion reaction, the anchoring of this stable catalyst on a stable silica support like SBA-15 results in an excellent hybrid material **5**, which performs as a true heterogeneous catalyst and can be recycled and reused up to at least five times without loss of activity. Its decreased activity (TOF 6 h^{-1}) as compared to that of its homogeneous counterpart (TOF 15 h^{-1}) is quite acceptable for an immobilized catalyst. The fact that in consecutive catalysis runs the structure and integrity of both organometallic moiety and the inorganic support persisted, nicely meets the objective set to merge properties of a homogeneous and a heterogeneous catalytic system into one sustainable hybrid catalyst.

Experimental Section

General Comments

3840). ^{13}C (188.6 MHz), ^{29}Si (149.0 MHz), and ^{31}P (303.7 MHz) CP/MAS NMR spectra of **5** were recorded on a Bruker AV-750 spectrometer (spinning rate 12 kHz, contact time for ^{13}C 2.048 ms, for ^{29}Si 10.24 ms, and for ^{31}P 2.048 ms; number of transients for ^{13}C 30916, for ^{29}Si 23484, and for ^{31}P 3920). FT-IR and DRIFT spectra were recorded using a Mattson Instruments Galaxy Series FTIR 5000 spectrometer with SPECAC diffuse-reflectance assembly or Perkin–Elmer Spectrum One FT-IR spectrometer with Universal ATR sampling accessory. Gas chromatographic analyses were performed with a Perkin–Elmer Autosystem XL GC using a 30 m, PE-17 capillary column with an FID detector. Microanalyses were obtained from H. Kolbe Mikroanalytisches Laboratorium, Mülheim an der Ruhr, Germany. Nitrogen physisorption was carried out at 77 K using a Micromeritics Tristar 3000 apparatus. The samples were dried in helium flow for 14 h at 393 K prior to analysis. The pore size distribution, micro- and mesoporosity were derived from the adsorption branch of the isotherm using an NL-DFT model developed by Jaroniec et al. for ordered mesoporous silica supports with cylindrical pore geometry.[29] The total pore volume was determined at $p/p_o = 0.995$, whereas the mesopore surface area was calculated with the t-method using a thickness range of 0.35–0.55 nm.[30] Powder X-ray diffraction (XRD) patterns of MCM-41 and hybrid material derived from it (**4**) were obtained from 1.5 to 10° 2θ with a Philips PW1710 setup using Cu-Kα radiation. XRD patterns of SBA-15 and hybrid materials derived from it (**3** and **5**) have been recorded using a Bruker-Nonius D8 Advance X-ray Diffractometer using Co-Kα$_1$ radiation. Electron microscopy analysis was performed using a Tecnai 20 microscope operating at 200 kV and equipped with an EDX detector.

Synthesis of MCM-41

MCM-41 was prepared according to a reported procedure.[31] Degussa Aerosil380 was used as silica source and the molar composition of the synthesis mixture was 1:0.27:0.19:40 (SiO$_2$:CTABr:TEAOH:H$_2$O).

Synthesis of SBA-15

SBA-15 was synthesized following a literature procedure.[25] An 8 g portion of EO$_{20}$PO$_{70}$EO$_{20}$ (P123) was dissolved in 250 mL demineralized water at 40°C. After the solution became clear, 48 g of concentrated HCl were added followed by addition of 21.5 mL of TEOS. Subsequently the mixture was stirred for 20 h at 40°C after which it was transferred to an oven for further reaction at 80°C for 48 h. The product was collected by filtration, dried in air for 12 h at 80°C, and calcined for 6 h at 540°C.

Grafting Procedure for Silica 3

In a typical procedure, 3 g of mesoporous silica (SBA-15) were pretreated by heating at 100°C under vacuum for 2 h. After being allowed to cool to room temperature, a solution of **1** (0.28 mmol) in dry toluene (100 mL) was introduced. The resulting mixture was stirred to form a suspension and heated at 90°C for 20 h, after which the silica was allowed to settle and the supernatant liquid was decanted. The silica was washed twice with dry CH$_2$Cl$_2$ (50 mL) and was subjected to Soxhlet extraction using CH$_2$Cl$_2$ for 16 h. Finally, it

was dried under vacuum affording 3.2 g of solid **3**. IR (KBr, DRIFT): $\tilde{v} = 3065, 2982, 2939, 2902$ (C−H, stretching); 1725 (C=O, stretching); 1514 (CHN group); 1438 cm^{-1} (N−H, bending); CP/MAS ^{13}C NMR (75.5 MHz, 25°C): $\delta = 8.62$ (SiCH_2), 16.68 (OCH$_2CH_3$), 29.4 (CH_2), 40.27 (ArCH_2P and NHCH_2), 58.61 (OCH_2), 121.69, 129.15, 131.57, 132.8, 141.65, 153.94, 157.57 (ArC), 160.59 (C=O); CP/MAS ^{31}P NMR (121.5 MHz, 25°C): $\delta = 36.01$; CP/MAS ^{29}Si NMR (59.6 MHz, 25°C): $\delta = -108.66, -101.34$; anal. found: C 4.96, P 0.85, Pd 0.82 (molar ratio of P/Pd = 2; found 3.6).

Grafting Procedure for Silica 4

Using **2** (15.2 mg, 0.021 mmol) and 0.5 g of MCM-41 gave 0.5 g of silica **4** in a similar procedure as for silica **3**. IR (KBr, DRIFT): $\tilde{v} = 2995, 2959, 2858$ (C−H, stretching); 1726 (C=O, stretching); 1465 (N−H, bending), 1395 cm^{-1}; CP/MAS ^{13}C NMR (75.5 MHz, 25°C): $\delta = 8.01$ (SiCH_2), 17.18 (OCH$_2CH_3$), 23.44 (CH_2), 42.0 (NHCH_2), 49.3 (ArCH_2S), 59.73 (OCH_2), 118.74, 127.29, 130.21, 132.63, 148.77, 152.11, 155.23, 162.95 (ArC), 165.45 (C=O); CP/MAS ^{29}Si NMR (59.6 MHz, 25°C): $\delta = -107.91, -99.64, -90.96$; anal. found: C 1.71, S 0.28, Pd 0.43; (molar ratio of S/Pd = 2; found 2.17).

Synthesis of Silica 5

2.37 g of silica **3** was suspended in a mixture of hexane (20 mL) and 1,1,1,3,3,3-hexamethyldisilazane (10 mL) and stirred at ambient temperature for 20 h, after which the silica was allowed to settle and the supernatant liquid was decanted. The silica was washed twice with dry CH$_2$Cl$_2$ (50 mL) and dried under vacuum yielding 2.2 g of solid **5**; IR (KBr, DRIFT): $\tilde{v} = 3063, 2963, 2905$ (C−H, stretching); 1756 (C=O, stretching); 1501 (CHN group); 1485, 1438 cm^{-1} (N−H, bending); CP/MAS ^{13}C NMR (188.64 MHz, 25°C): $\delta = -0.5$ (SiCH_3), 7.9 (SiCH_2), 17.1 (OCH$_2CH_3$), 22.6 (CH_2), 43.2 (ArCH_2P and NHCH_2), 58.8 (OCH_2), 117.5, 128.8, 132.6, 145.1 (ArC), 150.4 (C=O); CP/MAS ^{31}P NMR (303.7 MHz, 25°C): $\delta = 30.2$; CP/MAS ^{29}Si NMR (149.0 MHz, 25°C): $\delta = -108.2, -59.4, -52.1, -45.5, 13.9$; anal. found: C 7.66, P 0.58, Pd 0.57 (molar ratio of P/Pd = 2; found 3.4).

Catalysis

The catalytic experiments were carried out using *i*-Pr$_2$EtN (Hunig's base, 10 mol%) as a base, hybrid silica materials as catalyst (200–500 mg), and methyl isocyanoacetate (1.6 mmol) and benzaldehyde (1.6 mmol) as reagents in CH$_2$Cl$_2$ (5 mL) at room temperature. The reaction progress was monitored by means of GC analysis using pentadecane as internal standard. After each run, the complete reaction mixture was centrifuged and the supernatant was separated. The remainders were washed with CH$_2$Cl$_2$ (2×20 mL) and dried under vacuum. The obtained solid was used for the next run.

Acknowledgements

References

[1] B. Cornils, W. A. Herrmann, *J. Catal.* **2003**, *216*, 23–31; H.-U. Blaser, A. Indolese, A. Schnyder, *Curr. Sci.* **2000**, *78*, 1336–1344.

[2] P. McMorn, G. J. Hutchings, *Chem. Soc. Rev.* **2004**, *33*, 108–122; L.-X. Dai, *Angew. Chem. Int. Ed.* **2004**, *43*, 5726–5729; F. Quignard, A. Choplin, *Comprehensive Coordination Chemistry II* **2004**, Elsevier, San Diego, Oxford, Vol. 9, pp 445–470; D. J. Cole-Hamilton, *Science* **2003**, *299*, 1702–1706; F. R. Hartley, *Supported Metal Complexes*, Kluwer Academic, Dordrecht, **1985**.

[3] J. M. Thomas, R. Raja, *J. Organomet. Chem.* **2004**, *689*, 4110–4124.

[4] C. E. Song, S.-g. Lee, *Chem. Rev.* **2002**, *102*, 3495–3524; N. E. Leadbeater, M. Marco, *Chem. Rev.* **2002**, *102*, 3217–3274; Y. R. de Miguel, E. Brulé, R. G. Margue, *J. Chem. Soc., Perkin Trans. 1* **2001**, *23*, 3085–3094; Y. R. de Miguel, *J. Chem. Soc., Perkin Trans. 1* **2000**, *24*, 4213–4221; J. H. Clark, D. J. Macquarrie, *Chem. Commun.* **1998**, 853–860; A. Choplin, F. Quignard, *Coord. Chem. Rev.* **1998**, *178–180*, 1679–1702; D. Brunel, N. Bellocq, P. Sutra, A. Cauvel, M. Laspéras, P. Moreau, F. Di Renzo, G. Anne, F. François, *Coord. Chem. Rev.* **1998**, *178–180*, 1085–1108.

[5] P. M. Price, J. H. Clark, D. J. Macquarrie, *J. Chem. Soc., Dalton Trans.* **2000**, *2*, 101–110.

[6] M. E. van der Boom, D. Milstein, *Chem. Rev.* **2003**, *103*, 1759–1792; M. Albrecht, G. van Koten, *Angew. Chem. Int. Ed.* **2001**, *40*, 3750–3781.

[7] K. J. Szabo, *Synlett* **2006**, 811–824; S. Sebelius, V. J. Olsson, K. J. Szabo, *J. Am. Chem. Soc.* **2005**, *127*, 10478–10479; J. Kjellgren, J. Aydin, O. A. Wallner, I. V. Saltanova, K. J. Szabo, *Chem. Eur. J.* **2005**, *11*, 5260–5268; J. Kjellgren, H. Sunden, K. J. Szabo, *J. Am. Chem. Soc.* **2005**, *127*, 1787–1796; O. A. Wallner, K. J. Szabo, *J. Org. Chem.* **2005**, *70*, 9215–9221; J. Zhao, A. S. Goldman, J. F. Hartwig, *Science* **2005**, *307*, 1080–1082; O. A. Wallner, K. J. Szabo, *Org. Lett.* **2004**, *6*, 1829–1831; N. Solin, J. Kjellgren, K. J. Szabo, *J. Am. Chem. Soc.* **2004**, *126*, 7026–7033; N. Solin, O. A. Wallner, K. J. Szabo, *Org. Lett.* **2005**, *7*, 689–691; J. Kjellgren, H. Sunden, K. J. Szabo, *J. Am. Chem. Soc.* **2004**, *126*, 474–475; K. Takenaka, Y. Uozumi, *Org. Lett.* **2004**, *6*, 1833–1835; J. S. Fossey, C. J. Richards, *Organometallics* **2004**, *23*, 367–373; Z. Wang, M. R. Eberhard, C. M. Jensen, S. Matsukawa, Y. Yamamoto, *J. Organomet. Chem.* **2003**, *681*, 189–195; E. Diez-Barra, J. Guerra, V. Hornillos, S. Merino, J. Tejeda, *Organometallics* **2003**, *22*, 4610–4612; J. T. Singleton, *Tetrahedron* **2003**, *59*, 1837–1857; G. R. Rosa, G. Ebeling, J. Dupont, A. L. Monteiro, *Synthesis* **2003**, 2894–2897; I. G. Jung, S. U. Son, K. H. Park, K.-C. Chung, J. W. Lee, Y. K. Chung, *Organometallics* **2003**, *22*, 4715–4720; J. S. Fossey, C. J. Richards, *Tetrahedron Lett.* **2003**, *44*, 8773–8776; S. Sjoevall, O. F. Wendt, C. Andersson, *J. Chem. Soc., Dalton Trans.* **2002**, 1396–1400; G. Guillena, G. Rodriguez, G. van Koten, *Tetrahedron Lett.* **2002**, *43*, 3895–3898; J. M. Seul, S. Park, *J. Chem. Soc., Dalton Trans.* **2002**, 1153–1158; D. Morales-Morales, R. E. Cramer, C. M. Jensen, *J. Organomet. Chem.* **2002**, *654*, 44–50; J. A. Loch, M. Albrecht, E. Peris, J. Mata, J. W. Faller, R. H. Crabtree, *Organometallics* **2002**, *21*, 700–706; B. S. Williams, P. Dani, M. Lutz, A. L. Spek, G. van Koten, *Helv. Chim. Acta* **2001**, *84*, 3519–3530; S. Gruendemann, M. Albrecht, J. A. Loch, J. W. Faller, R. H. Crabtree, *Organometallics* **2001**, *20*, 5485–5488; J. Dupont, M. Pfeffer, J. Spencer, *Eur. J. Inorg. Chem.* **2001**, 1917–1927; D. Morales-Morales, C. Grause, K. Kasaoka, R. Redon, R. E. Cramer, C. M. Jensen, *Inorg. Chim. Acta* **2000**, *300–302*, 958–963; D. Morales-Morales, R. Redon, C. Yung, C. M. Jensen, *Chem. Commun.* **2000**, 1619–1620; M. A. Stark, G. Jones, C. J. Richards, *Organometallics* **2000**, *19*, 1282–1291; R. A. Gossage, J. T. B. H. Jastrzebski, J. van Ameijde, S. J. E. Mulders, A. J. Brouwer, R. M. J. Liskamp, G. van Koten, *Tetrahedron Lett.* **1999**, *40*, 1413–1416; R. A. Gossage, L. A. van de Kuil, G. van Koten, *Acc. Chem. Res.* **1998**, *31*, 423–431; X. Zhang, J. M. Longmire, M. Shang, *Organometallics* **1998**, *17*, 4374–4379; M. Ohff, A. Ohff, M. E. van der Boom, D. Milstein, *J. Am. Chem. Soc.* **1997**, *119*, 11687–11688; S. E. Denmark, R. A. Stavenger, A.-M. Faucher, J. P. Edwards, *J. Org. Chem.* **1997**, *62*, 3375–3389; F. Gorla, A. Togni, L. M. Venanzi, A. Albinati, F. Lianza, *Organometallics* **1994**, *13*, 1607–1616.

[8] G. Rodriguez, M. Lutz, A. L. Spek, G. van Koten, *Chem. Eur. J.* **2002**, *8*, 45–57.

[9] C. Schlenk, A. W. Kleij, H. Frey, G. van Koten, *Angew. Chem. Int. Ed.* **2000**, *39*, 3445–3447.

[10] D. E. Bergbreiter, P. L. Osburn, Y.-S. Liu, *J. Am. Chem. Soc.* **1999**, *121*, 9531–9538.

[11] M. Q. Slagt, S.-E. Stiriba, H. Kautz, R. J. M. Klein Gebbink, H. Frey, G. van Koten, *Organometallics* **2004**, *23*, 1525–1532; M. Q. Slagt, S.-E. Stiriba, R. J. M. Klein Gebbink, H. Kautz, H. Frey, G. van Koten, *Macromolecules* **2002**, *35*, 5734–5737; A. W. Kleij, R. A. Gossage, J. T. B. H. Jastrzebski, J. Boersma, G. van Koten, *Angew. Chem. Int. Ed.* **2000**, *39*, 176–178.

[12] D. E. Bergbreiter, S. Furyk, *Green Chem.* **2004**, *6*, 280–285.

[13] B. M. J. M. Suijkerbuijk, L. Shu, R. J. M. Klein Gebbink, A. D. Schlueter, G. van Koten, *Organometallics* **2003**, *22*, 4175–4177.

[14] M. Q. Slagt, J. T. B. H. Jastrzebski, R. J. M. Klein Gebbink, H. J. van Ramesdonk, J. W. Verhoeven, D. D. Ellis, A. L. Spek, G. van Koten, *Eur. J. Org. Chem.* **2003**, 1692–1703; A. W. Kleij, R. J. M. Klein Gebbink, P. A. J. van den Nieuwenhuijzen, H. Kooijman, M. Lutz, A. L. Spek, G. van Koten, *Organometallics* **2001**, *20*, 634–647; A. W. Kleij, R. A. Gossage, R. J. M. Klein Gebbink, N. Brinkmann, E. J. Reijerse, U. Kragl, M. Lutz, A. L. Spek, G. van Koten, *J. Am. Chem. Soc.* **2000**, *122*, 12112–12124.

[15] H. P. Dijkstra, C. A. Kruithof, N. Ronde, R. van de Coevering, D. J. Ramon, D. Vogt, G. P. M. van Klink, G. van Koten, *J. Org. Chem.* **2003**, *68*, 675–685; H. P. Dijk-

stra, N. Ronde, G. P. M. van Klink, D. Vogt, G. van Koten, *Adv. Synth. Catal.* **2003**, *345*, 364–369; H. P. Dijkstra, G. P. M. van Klink, G. van Koten, *Acc. Chem. Res.* **2002**, *35*, 798–810.

[16] R. van de Coevering, A. P. Alfers, J. D. Meeldijk, E. Martinez-Viviente, P. S. Pregosin, R. J. M. Klein Gebbink, G. van Koten, *J. Am. Chem. Soc.* **2006**, *128*, 12700–12713; R. van de Coevering, M. Kuil, R. J. M. Klein Gebbink, G. van Koten, *Chem. Commun.* **2002**, 1636–1637.

[17] D. E. Bergbreiter, *Chem. Rev.* **2002**, *102*, 3345–3384; D. E. Bergbreiter, P. L. Osburn, J. D. Frels, *J. Am. Chem. Soc.* **2001**, *123*, 11105–11106.

[18] N. C. Mehendale, C. Bezemer, C. A. van Walree, R. J. M. Klein Gebbink, G. van Koten, *J. Mol. Catal. A* **2006**, *257*, 167–175.

[19] R. Gimenez, T. M. Swager, *J. Mol. Catal. A:* **2001**, *166*, 265–273.

[20] K. Yu, W. Sommer, J. M. Richardson, M. Weck, C. W. Jones, *Adv. Synth. Catal.* **2005**, *347*, 161–171; W. Sommer, K. Yu, J. S. Sears, Y. Ji, X. Zheng, R. J. Davis, C. D. Sherrill, C. W. Jones, M. Weck, *Organometallics* **2005**, *24*, 4351–4361; K. Yu, W. Sommer, M. Weck, C. W. Jones, *J. Catal.* **2004**, *226*, 101–110; R. Chanthateyanonth, H. Alper, *Adv. Synth. Catal.* **2004**, *346*, 1375–1384; R. Chanthateyanonth, H. Alper, *J. Mol. Catal. A:* **2003**, *201*, 23–31.

[21] N. C. Mehendale, R. W. A. Havenith, M. Lutz, A. L. Spek, R. J. M. Klein Gebbink, G. van Koten, *manuscript in preparation*.

[22] N. C. Mehendale, M. Lutz, A. L. Spek, R. J. M. Klein Gebbink, G. van Koten, *manuscript in preparation*.

[23] N. C. Mehendale, M. Lutz, A. L. Spek, R. J. M. Klein Gebbink, G. van Koten, *manuscript in preparation*.

[24] C. T. Kresge, M. E. Leonowicz, W. J. Roth, J. C. Vartuli, J. S. Beck, *Nature* **1992**, *359*, 710–712.

[25] D. Zhao, J. Feng, Q. Huo, N. Melosh, G. H. Fredrickson, B. F. Chmelka, G. D. Stucky, *Science* **1998**, *279*, 548.

[26] J. R. A. Sietsma, J. D. Meeldijk, J. P. Den Breejen, M. Versluijs-Helder, A. J. Van Dillen, P. E. De Jongh, K. P. De Jong, *Angew. Chem. Int. Ed.* **2007**, *46*, 4547–4549; A. Sakthivel, J. Zhao, M. Hanzlik, A. S. T. Chiang, W. A. Herrmann, F. E. Kuehn, *Adv. Synth. Catal.* **2005**, *347*, 473–483; N. K. K. Raj, S. S. Deshpande, R. H. Ingle, T. Raja, P. Manikandan, *Catal. Lett.* **2004**, *98*, 217–224; V. Ayala, A. Corma, M. Iglesias, F. Sanchez, *J. Mol. Catal. A:* **2004**, *221*, 201–208; J. V. Nguyen, C. W. Jones, *Macromolecules* **2004**, *37*, 1190–1203; H. Ma, J. He, D. G. Evans, X. Duan, *J. Mol. Catal. B:* **2004**, *30*, 209–217; C. González-Arellano, A. Corma, M. Iglesias, F. Sánchez, *Adv. Synth. Catal.* **2004**, *346*, 1316–1328; P. N. Liu, P. M. Gu, F. Wang, Y. Q. Tu, *Org. Lett.* **2004**, *6*, 169–172; P. Stepnicka, J. Demel, J. Cejka, *J. Mol. Catal. A:* **2004**, *224*, 161–169; J.-H. Kim, G.-J. Kim, *Catal. Lett.* **2004**, *92*, 123–130.

[27] T. Maschmeyer, F. Rey, G. Sankar, J. M. Thomas, *Nature* **1995**, *378*, 159–162.

[28] M. W. McKittrick, C. W. Jones, *J. Catal.* **2004**, *227*, 186–201.

[29] M. Jaroniec, M. Kruk, J. P. Olivier, S. Koch, *Stud. Surf. Sci. Catal.* **2000**, *128*, 71–80.

[30] B. C. Lippens, J. H. De Boer, *J. Catal.* **1965**, *4*, 319–323.

[31] C.-F. Cheng, D. H. Park, J. Klinowski, *J. Chem. Soc., Faraday Trans.* **1997**, *93*, 193–197.